21 March 1980, Volume 207, Number 4437 SCIENCE

Neutral Beam Heating in the Princeton Large Torus

L. R. Grisham

Begun in the early 1950's, the controlled thermonuclear fusion program was born out of the dream of tapping the energy source that drives the stars, to provide relatively safe and almost limitless power as long as man endures. Of the numerous magnetic confinement topologies explored since that time, the tokamak's (1) is the one that has received the most study over the past decade. The tokamak presently appears to offer the most immediate, although not the only, hope of eventually leading to a practical electricity-producing fusion reactor. Pioneered at the I. V. Kurchatov Institute in the Soviet Union during the 1950's, tokamaks first appeared in the United States in 1969 with the commissioning of the ST tokamak (2) at Princeton University. This was followed rapidly by tokamaks at Oak Ridge National Laboratory, Massachusetts Institute of Technology, the University of Texas, and the General Atomic Company in San Diego.

Summary. Beams of energetic atoms were injected to heat the plasma contained in the Princeton Large Torus tokamak. The plasma reached ion temperatures of about 6.5 kiloelectron volts ($\approx$ 75 million K) and electron temperatures of about 4.0 kiloelectron volts or greater ($\approx$ 46 million K)—both the highest yet achieved in a tokamak device. Although a new type of density fluctuation in the plasma was observed at the highest injection powers and lowest plasma densities, the energy confinement properties of the discharge did not appear to deteriorate even at the low collisionalities relevant to a thermonuclear reactor plasma. The electron energy confinement in the central plasma appeared to be enhanced during beam injection.

This article discusses recent experiments on the efficacy of plasma heating by the injection of energetic neutral beams; these experiments were carried out on the Princeton Large Torus (PLT) tokamak at the Princeton University Plasma Physics Laboratory by the members of the PLT and the Neutral Injection groups. Previous neutral beam injection experiments on the CLEO (3), ATC (4), ORMAK (5), TFR (6), DITE (7), and T-11 (8) tokamaks demonstrated substantial ion heating, reaching central ion temperatures, $T_i(0)$, of as much as ~ 2 kiloelectron volts. The recent PLT experiments achieved, during 1978, the highest temperatures to date on a tokamak (central ion and central electron temperatures of ≈ 6.5 and $\gtrsim 4.0$ keV, respectively), reaching for the first time the ion temperatures at which a fusion reactor begins to be feasible.

The author is a physicist in the Neutral Injection group at the Princeton University Plasma Physics Laboratory, Princeton, New Jersey 08544. The research discussed in this article was carried out by the members of the Princeton Large Torus (PLT) group, headed by W. Stodiek, and the Neutral Injection group, headed by H. P. Eubank. This article is partially based on papers presented by the PLT and Neutral Injection groups at the 7th International Conference on Plasma Physics and Controlled Nuclear Fusion Research, Innsbruck, Austria, 23 to 30 August 1978 and (17).

The Princeton Large Torus Tokamak

Figure 1 shows the rudiments of the PLT tokamak. The plasmas produced in this device have a major radius, R_0, of 134 centimeters and a minor radius, a, of 40 centimeters. The annular coils surrounding the vacuum vessel produce a 32-kilogauss toroidal (Φ direction) magnetic field that is stronger toward the inside of the torus and weaker toward the outside. After the initiation of a cool low-density plasma in the vacuum vessel by a radio-frequency oscillator, an electric field is induced around the torus by an air core transformer, with the toroidal plasma acting as the secondary winding. The toroidal electric current driven by this field gives rise to a poloidal (θ direction) magnetic field that is much weaker than the toroidal one and varies with minor radius, depending on the distribution of current within the plasma. Superposition of the toroidal and poloidal fields results in a sheared helical magnetic field, along which the ions and electrons of the plasma are constrained to spiral. In the absence of magnetic perturbations, all the field lines are at least asymptotically closed, in that each field line defines and fills up a particular toroidal surface. Thus, barring the effects of collisions, charged particle trajectories are closed within the plasma.

A purely toroidal magnetic field would, of course, also have closed field lines. Such a field would not, however, effectively contain a plasma, because the gradient in the toroidal magnetic field induces a vertical drift of positively and negatively charged particles in opposite directions. The vertical electric field associated with the resulting charge separation, coupled with the toroidal magnetic field, gives rise to a radial drift directed outward from the major axis for particles of both polarities, with the consequence that the plasma would be expelled on a time scale of about 10^{-6} second. The addition of the poloidal field due to the plasma current circumvents this problem, since electrical conduction along the helical field lines "shorts out" the charge separation. A particle following a helical field line spends its time equally above and below the midplane of

0036-8075/80/0321-1301$02.00/0

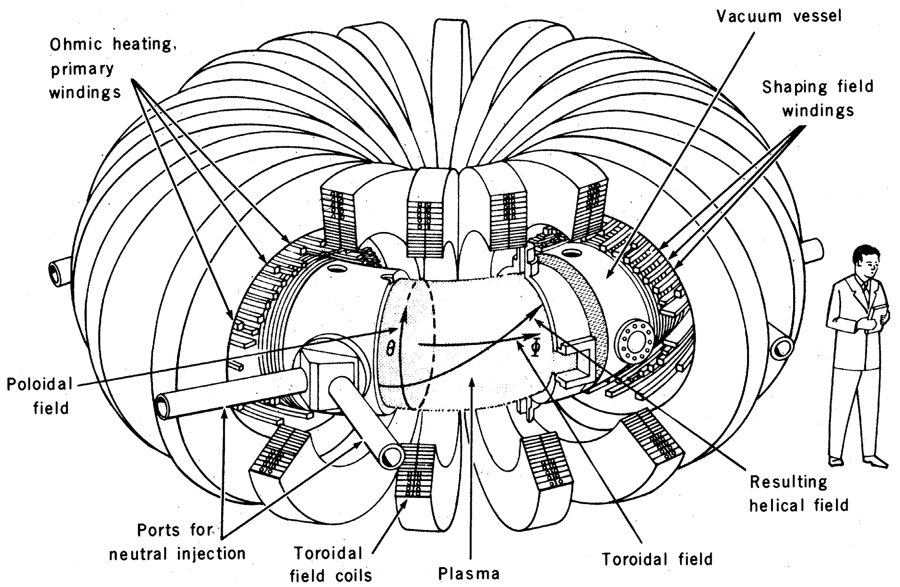

Fig. 1. Diagram of the PLT tokamak. The annular toroidal field coils produce the toroidal magnetic field in the Φ direction. The current flowing in the plasma creates the poloidal magnetic field in the θ direction. The resulting magnetic field has helical lines.

the torus, with the consequence that its drift, which is always in the same vertical direction, is cancelled.

Besides producing the poloidal magnetic field, the toroidal current heats the plasma through collisions between the plasma particles—that is, ordinary resistive or ohmic heating. Implicit in the tokamak concept, ohmic heating has been employed in all such devices, either alone or in conjunction with other heating methods. Since the Coulomb collision cross section falls as the inverse of the square of the particle energy, the plasma resistivity necessarily declines with increasing temperature, and the concomitant drop in dissipated power renders ohmic heating largely ineffective above temperatures of 1 to 2 keV (1 keV = 11,605,000 K). Inasmuch as an operating deuterium-tritium fusion reactor would require temperatures in the range of ~10 keV, the falling efficacy of ohmic heating dictates the use of alternative heating methods. Of these, neutral beam injection is one of the best understood, and has recently undergone the most development.

Neutral Injectors

The principle of neutral injection is elegantly simple: A beam of particles—atomic or "neutral" in order to cross the magnetic fields surrounding the plasma, and energetic enough to penetrate well inside the plasma periphery before being ionized—is injected into the tokamak. Since the purpose is to heat—that is, supply energy rather than particles to the plasma—the energy of the injected neutrals must be well above the mean thermal energy of the background plasma particles. In practice, selection of the energy to be used is based primarily on achieving adequate penetration, which automatically satisfies the heating condition. Inside the plasma, the beam neutrals are ionized (largely by charge exchange and impact ionization with the plasma ions), and the resulting beam ions travel along the magnetic field lines, colliding with the plasma particles in the process and transferring energy. Barring subsequent charge exchange and loss from the plasma as neutrals, or large orbit excursions out of the plasma, these beam ions continue to lose energy to the background plasma until they reach the ambient ion temperature—that is, are thermalized. Provided the injected neutrals have sufficient energy to reach the plasma center, the resultant energy deposition profile may be peaked on or near the axis. Unlike ohmic heating, neutral beam injection is not temperature-restrained; at higher temperatures the beam ions simply take longer to thermalize, but they nonetheless heat the plasma effectively.

No existing beam systems are capable of the voltage and power needed for a full-size thermonuclear reactor. However, the technology of producing intense neutral beams at appropriate energies has evolved rapidly, and systems now available are an order of magnitude more powerful than those of a decade ago. Programs at a number of laboratories are developing beams suitable for larger tokamaks of the future. The neutral injectors that were used in the PLT experiments were developed and built by the Plasma Technology Section of the Fusion Energy Division at Oak Ridge National Laboratory.

Figure 2 is a schematic of a neutral injector. A reflex arc is used to form a plasma, from which ions are electrostatically extracted and accelerated through ~2000 circular apertures in a set of grids. In normal operation, grid 1 and the arc chamber are at a potential of about +40 kilovolts, grid 2 is at about −1.3 kilovolts, and grid 3 is at ground potential. The resultant potential distribution not only accelerates the ions, but also maintains a potential barrier, preventing electrons produced in the neutralizer cell from being accelerated back into the source. While traversing the neutralizer cell (a gas conductance-limiting cylinder), the ions exchange charge with the gas streaming from the arc chamber. The fraction of beam particles that emerge from the neutralizer as neutrals is governed by the relative magnitudes of the ionization and neutralization cross sections. At 40 keV, the theoretical equilibrium fraction of neutrals is approximately 70 percent for H, and the PLT injectors normally achieve more than 60 percent. After the neutralizer, the remaining ions are magnetically deflected onto water-cooled beam dumps, while the neutrals continue down a duct into the tokamak. To limit gas flow into the torus, each injector is pumped by liquid helium-charged cryocondensation panels with an effective speed of ≈ 300,000 liters per second.

The PLT is equipped with four neutral injectors tangential to the plasma axis. Two fire parallel to the plasma current direction (coinjectors) and two fire antiparallel (counterinjectors). The maximum power injected by the system so far has been 2.4 megawatts of deuterium at 38 to 40 kV in 150-millisecond pulses.

Princeton Large Torus Operations

The PLT, like most other tokamaks, relies on a material limiter to demarcate the edge of the plasma. Although ordinarily touched by only the comparatively cool plasma periphery, the limiter suffers considerable power loading and particle bombardment, and can introduce impurities into the plasma through sputtering or evaporation. Accordingly, the limiter composition is of paramount importance. Any impurity tends to increase energy loss from the plasma through enhanced radiation; the most severe energy loss arises from ultraviolet line transitions of bound states. Light impurities tend to "burn out" in the hot central plasma, where they become completely stripped of electrons. Heavy impurities are more pathological, in that they tend to retain some bound electrons even at electron temperatures, T_e, of several kiloelectron volts and hence radiate energy prodigiously from the plasma core. This energy is, in turn, supplied by collisions with free electrons, which are therefore cooled by the process. Central radiation circumvents the magnetic confinement by providing a direct-loss channel for energy from the electrons in the hot reacting core. This loss is in parallel with the diffusion, conduction, and convection losses of the confined particles. Peripheral radiation, on the other hand, ejects from the edge plasma energy that has already escaped from the center, and therefore it is effectively in series with the core energy confinement.

During preliminary injector operation the PLT limiters were made of tungsten, chosen because of its high melting point and low sputtering yield. However, the tungsten quasi-continuum radiation (50 to 100 angstroms) from the plasma core quenched the electron temperature rise, particularly when counterinjection was used, and at low plasma densities the central electron temperatures, $T_e(0)$, even fell. Subsequently, and throughout the experiments discussed below, limiters of water-cooled graphite or stainless steel were employed. Even the components of stainless steel, which have considerably lower atomic numbers, proved troublesome, but the graphite limiters were quite successful. A comparison of power emanation profiles, obtained by Abel inversion of multichord scans with a bolometer, showed central peaking of the emitted power during injection in the presence of steel limiters and peripheral peaking during injection with the graphite limiters. The graphite thus appears superior, since radiation at the edge is much less deleterious to the gross energy confinement, and the greatly reduced axial power loss bounds $T_e(0)$ less stringently.

Initial injector operation was accompanied by large plasma density increases, which impeded temperature increases through sheer dilution. Much of this gas evolved from the vacuum vessel wall; evidently gas that had left the discharge was being recycled more rapidly due to the input beam power. This phenomenon has been controlled by introducing three sublimation balls, which deposit fresh layers of titanium onto most of the vacuum vessel wall between discharges. Acting as a getter, the fresh

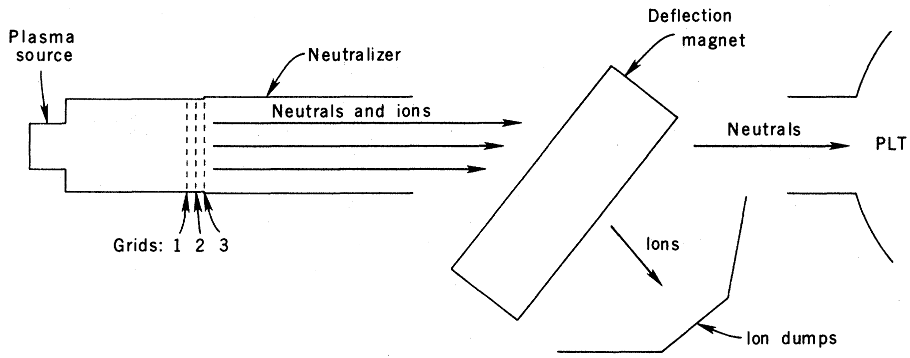

Fig. 2. Functional diagram of a neutral injector. Ions from the source plasma are electrostatically accelerated through the grids and partially neutralized in the neutralizer gas cell. The remaining ions are magnetically deflected, leaving the neutral atoms to enter the tokamak plasma.

titanium traps neutral hydrogen and impurity atoms emerging from the plasma. In combination with a feedback-controlled gas supply system, the gettering has made it possible to limit increases of $\bar{n}_e$, the line-averaged electron density across a minor diameter, to 1×10^{13} electrons per cubic centimeter or less during injection. This represents an increase in the total number that is comparable to the direct input of energetic beam particles.

Plasma Temperature

At moderate plasma densities in the PLT, the collisional equilibration of ion and electron temperatures proceeds more slowly than energy loss from the plasma. Consequently, the ion and electron temperatures are not constrained to be identical, and in general they are not, since heating methods are somewhat selective as to which species they heat. Ohmic heating, for example, heats the electrons, which in turn transfer energy to the ions through collisions as long as the ions are colder. Neutral beams, on the other hand, give more energy to the ions than the electrons, provided the initial energy of the injected beam is less than about 35 kT_e, where k is the Boltzmann constant.

Ion Heating Measurements and Results

Plasma temperatures, which typically range into the millions of degrees, clearly defy measurement by pedestrian means. There are, however, a number of techniques that are applicable to hot plasmas, all of which depend, more or less directly, on the fact that the average velocities of the ions and electrons comprising the plasma are necessarily greater the higher the temperature. Each measurement technique is characterized by different limitations and uncertainties. Thus, where possible, we use more than one method to diagnose the temperature, since agreement between different measurements enhances our confidence in the results. Three independent techniques are used on the PLT to determine the ion temperature, T_i: charge exchange measurements, neutron emission measurements, and measurements of the Doppler broadening of impurity line radiation.

The charge exchange method determines the ion temperature from the energy distribution of the fast neutrals that are created through charge exchange events in the plasma core and escape from the discharge. With mass separation, this method can measure the neutral flux from the bulk ion species at energies of 1.5 to 7 times $T_i(0)$, uncontaminated by slowing-down beam ions, provided the neutral beams and bulk plasma consist of different hydrogen isotopes. The most significant uncertainty in this measurement arises from the possibility that neutral beam injection might distort the thermal ion distribution, producing an increase in the high-energy tail of the Maxwellian, which would tend to artificially elevate the measured temperature. A linearized calculation of this effect for the CLEO tokamak injection experiment (*9*) predicted substantial distortion when it was simply extrapolated to PLT injection parameters. However, our numerical calculations based on the nonlinear Fokker-Planck equation (*10*) predict no significant departure from a Maxwellian distribution. These two analyses differ primarily in the implied energy flows. The CLEO calculation assumed that all the energy transferred by the beam ions to the high-energy tail particles was coupled solely to the bulk ion distribution, and further that all the tail particles had lower velocities than the beam ions. In the PLT plasma, however, both these assumptions are violated. The tail particles thermalize among themselves, and the energy deposited from the beam is also transferred from the tail ions to the electrons by ion-electron scattering, as well as carried away by ion thermal conduction and lost through particle diffusion and charge exchange. Moreover, some tail particles have higher velocities than the beam ions. For injection of 40-keV D^0 into an H^+ plasma, H^+ tail ions with energies $E > 10$ keV have higher velocities than the average slowing-down beam ion. In our nonlinear calculation, where neutral beam heating is balanced against ion-electron coupling and a relatively energy-insensitive loss process such as charge exchange, the bulk ion distribution is able to thermalize quite well, and little distortion occurs. Consequently, the charge exchange measurements should reflect the true central bulk ion temperature, a conclusion that is supported by the measured neutral fluxes, which indicate no strong departure from a Maxwellian ion energy distribution.

The strong energy dependence of the D-D fusion cross section makes the resulting neutron flux a sensitive measure of the temperature of the reacting deuterons. However, during injection of D^0 beams into a D^+ plasma, the neutrons resulting from reactions of the slowing-down beam ions, with each other and with the thermal deuterons, mask those arising from purely thermal reactions. This is not a problem during injection of H^0 beams into a D^+ plasma, and for these cases the neutron emission is used to deduce the central ion temperature. As with the charge exchange method, the accuracy of this measurement could be compromised if the bulk ion energy distribution function were seriously distorted. However, nonlinear numerical calculations again indicate a negligible effect on the inferred ion temperature. The early history of measurements of neutrons from fusion devices was fraught with difficulties, the greatest of which was the nonthermonuclear origin of many of the neutrons (*11*). In the present experiments, however, there is no statistically significant energy shift between the neutron spectra arising from strictly coinjection and strictly counter-injection of H^0 into a D^+ plasma. This indicates that the average center-of-mass velocity of the pairs of reacting deuterons is nil, and is consistent with a thermonuclear origin of the neutrons (*12*). A remaining uncertainty arises from the unknown plasma composition during H^0 injection into a low-density, initially D^+ plasma. Although for these cases the total density increase is ~ 50 percent

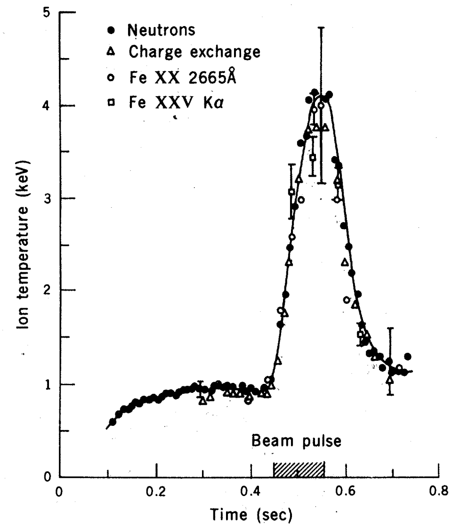

Fig. 3. Ion temperature of the central PLT plasma measured in four ways. The neutral beams inject ≈ 1.6 MW of power over the interval 0.45 to 0.55 second. The target plasma was D^+, with $\bar{n}_e = 2.2 \times 10^{13}$ cm^{-3} at the end of injection, and the beams were H^0.

greater than the beam particle influx, the density increase on axis is more than accounted for by the injected ions. To study the composition of the neutron-emitting plasma core under such conditions, we performed the inverse injection experiment—injecting D^0 into an H^+ plasma. By measuring the neutron flux after the beam pulse was turned off and the beam ions had thermalized, and knowing the ion temperature from other measurements, we could infer the increase in deuterium on the axis. We found that the injected ion density approximately accounted for the density increase on the axis during injection. The uncertainty in this plasma composition measurement does, however, result in large errors (~ 20 percent) in the neutron-deduced T_i.

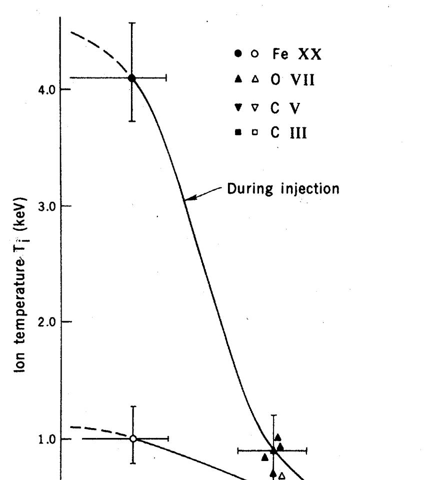

Fig. 4. Radial profile of ion temperature from Doppler broadening of impurity lines before and after injection of ≈ 1.6 MW of H^0 into a D^+ plasma; $\bar{n}_e = 2.2 \times 10^{13}$ cm^{-3} at the end of injection.

The ion temperature is also determined by measurements of the Doppler broadening of impurity lines. A forbidden line of Fe(XX) has been identified at 2665.1 Å, and its Doppler width is used as a measure of the near-central ion temperature, since experimentally the Fe(XX) radiation peaks at radius $r \lesssim 10$ cm even in discharges with $T_e(0) = 3$ keV. At the highest ion temperatures we are also able to use ultraviolet radiation from Fe(XXIV) for measurements closer to the plasma center. In addition, an x-ray crystal spectrometer is used to measure broadening of the $1s$-$2p$ transition of Fe(XXV) at 1.85 Å, which should be emitted from a very narrow region in the hot plasma core.

Unlike the charge exchange and neutron flux measurements, the Doppler broadening measurements are insensitive to distortions of the bulk ion distribution function. The impurity ion temperature, however, may not precisely equal that of the bulk ion species. Since the coupling mechanism between the beam and plasma ions is Coulomb scattering, the power input to each plasma ion species scales as $n_i Z_i^2 / m_i$, where Z_i is the charge of the species, n_i its density in the plasma, and m_i its mass. Highly stripped impurity species thus receive more beam power per ion than does the bulk plasma of H^+ or D^+. At low densities and high ion temperatures, collisions between the impurity ions and hydrogenic species become sufficiently infrequent that the differential power input should result in a measurable difference in temperatures. At the highest beam powers, and lowest plasma densities, this effect can account for a 25 percent temperature differential. However, our calculations indicate that for cases with $T_i(0) \leq 4$ keV in the PLT, the temperature difference due to this effect should be within the experimental accuracy of the measurements.

Figure 3 shows the ion temperature in the plasma core of a D^+ discharge into which a total of 1.6 MW of H^0 was injected for 100 msec. It is notable that the temperatures deduced from the neutron flux, charge exchange flux, and Doppler broadening of two separate iron lines are all in good agreement. For these cases $\bar{n}_e$ was 2.2×10^{13} cm^{-3} at the end of injection. The sharp rise in T_i during the beam pulse is readily apparent. Figure 4 shows a radial profile of T_i before and during in-

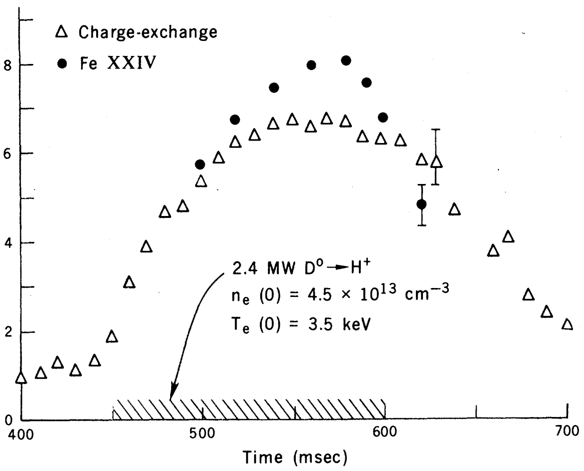

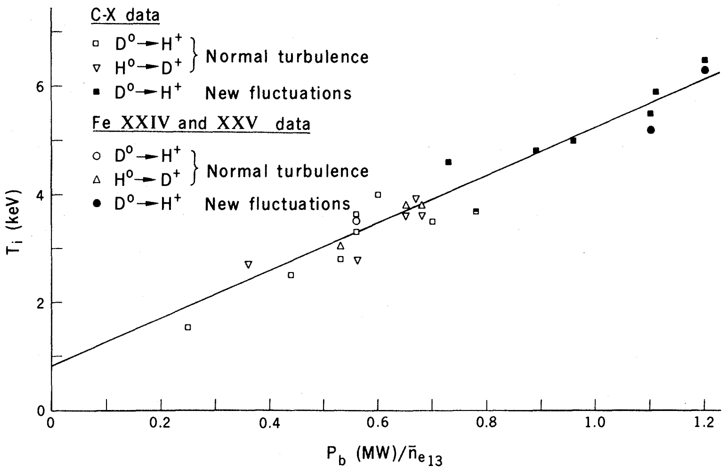

Fig. 5 (left). Central ion temperature with injection of ≈ 2.4 MW of D^0 into an H^+ plasma with $\bar{n}_e = 2 \times 10^{13}$ cm^{-3}. The measurements are from the energy distribution of hydrogen neutrals and from the Doppler broadening of an Fe(XXIV) line. The temperature of the Fe is predicted to be about 1700 eV above that of the H. Fig. 6 (right). Ion temperature increase versus beam power per unit plasma density. Linearity persists well into the regime where the new type of density fluctuations appear.

jection for the same case as Fig. 3, obtained by extending the Doppler broadening measurements to lines of light impurities, which radiate primarily in the outer plasma. It is apparent that, as desired, the neutral injection is effecting a greater relative increase in the ion temperature in the center of the plasma than on the edge.

The maximum power injected during these experiments was 2.4 MW of D^0 into an H^+ plasma with $\bar{n}_e = 2 \times 10^{13}$ cm^{-3}. Under these conditions, $T_i(0)$ reached 6.5 keV and $T_e(0)$ reached 4.0 keV. Figure 5 shows T_i as a function of time deduced from the H^0 charge exchanged flux for this case, as well as the corresponding temperatures of Fe(XXIV) ions from Doppler broadening measurements. Calculations indicate that for these conditions the temperature of the iron impurity ions should be about 1700 eV above that of the H^+ ions, which puts the 8.1-keV iron temperature in quite good agreement with the 6.6-keV H^0 charge exchange temperature. The central electron density in this case was 5×10^{13} cm^{-3}.

Ion Collisionality

Figure 6 illustrates the dependence of the increase in the central ion temperature on the injected power per unit density. We studied the transmission and scattering of microwave energy and the emission of soft x-ray photons to monitor the turbulence that is normally present in the plasma. At lower values of $P_b/\bar{n}_e$ (where P_b is beam power) the amplitude of small-scale density fluctuations is increased by a factor of ≤ 3 (indicated by the open data points in Fig. 6). With greater beam power per unit density, however, a new form of oscillation appears in a frequency range near 100 kHz, which is normally quiescent. The filled data points in Fig. 6 indicate the presence of these new fluctuations. The mode structure and plasma transport due to these fluctuations have not been determined; however, it is significant and reassuring that the slope of the data is unchanged after their onset. It has been established that these new fluctuations occur at higher T_i and lower densities, which correspond to lower values of the ion collisionality parameter $\nu_i{}^*$, and higher values of $P_b/\bar{n}_e$.

The collisionality parameter is an important measure of the approach toward reactor conditions. A particle gyrating along one of the helical magnetic field lines in a tokamak experiences alternating maxima and minima of the field strength as its orbit takes it from inside to outside the minor axis of the torus. The relatively weak magnetic wells formed between successive maxima trap particles that have a sufficiently small component of their velocity parallel to the field. The trapped particles are reflected by the stronger magnetic field and, instead of circulating continuously around the torus, they bounce back and forth between their reflection points at a characteristic "bounce frequency." The projections on a plane of constant toroidal angle of the orbits thus described assume a characteristic banana shape, due to the vertical drift engendered by the radial gradient of the magnetic field. The portion of phase space occupied by trapped particles is given approximately by $\sqrt{2r/R_0}$. However, particles can be scattered off banana orbits by binary Coulomb encounters with other particles in the plasma. The dimensionless parameter $\nu_i{}^*$ is the frequency of detrapping by Coulomb scattering divided by the bounce frequency.

If the detrapping frequency is greater than the bounce frequency ($\nu_i{}^* > 1$), the particles on the average do not remain in a trapped orbit long enough to complete a bounce. If the detrapping frequency is less than the bounce frequency ($\nu_i{}^* < 1$), the particles on the average are able to trace out complete banana orbits, and under such conditions the plasma is referred to as collisionless. The collisionality of the plasma is important for two reasons. First, the classical collisional diffusion process is enhanced by a substantial factor when particles are able to form complete banana orbits, since these orbits result in radial excursions large compared to those of untrapped orbits. Second, and more importantly, a variety of new instabilities—collective phenomena involving sympathetic oscillations of many particles to form waves in the plasma—are predicted to occur under collisionless conditions, where the velocity-randomizing effects of collisions are insufficient to quench collective modes coupled to the ion or electron bounce motion. The diffusion associated with instabilities, called anomalous because it is not in agreement with collisional diffusion theory, is predicted on the basis of simple considerations to be much faster in tokamaks than "neoclassical" diffusion (*13*) (which includes only diffusion of trapped and untrapped particles due to binary Coulomb collisions), deep in the trapped ion or low-collisionality regime where fusion reactors are expected to operate. However, it is extremely difficult to predict whether these instabilities will saturate before they seriously affect the transport of energy out of the plasma. Since previous tokamaks operated in regimes with $\nu_i^* > 1$, the significance of these instabilities has been uncertain, and whether instability-enhanced anomalous diffusion or the more optimistic neoclassical theory would more accurately describe ion thermal conduction in the trapped ion regime has been unknown.

At the highest temperatures and lowest densities for which data are shown in Fig. 6, ν_i^* over most of the plasma is less than 0.1 (it has a minimum of ~ 0.02) and is thus well into the trapped ion regime relevant to reactors. The expected error in ν_i^* due to uncertainties about impurity levels is thought to be no greater than a factor of 2. The approximate constancy of the slope of Fig. 6, despite the low collisionality and the onset of the new fluctuations, indicates that whatever new instabilities may occur in the collisionless plasma, they are not yet significantly deleterious to the ion energy confinement.

Electron Heating

The electron temperature is measured in several ways: from the Doppler broadening of Thompson-scattered ruby laser light, from microwave emission at the electron cyclotron frequency ω_{ce}, and from far-infrared radiation at $2\omega_{ce}$. Although the increases in T_e due to neutral injection are not as large as those in T_i, we do achieve significant electron heating. The different measuring techniques indicate temperatures that are generally in reasonably good agreement with each other. Figure 7 shows measurements of the time variation of T_e at selected radii as determined by the $2\omega_{ce}$ emission. Corresponding to magnetohydrodynamic fluctuations in the central plasma, the long-period sawteeth ($\Delta T_e \sim 300$ eV) are common in tokamak plasmas, and a frequent but not ubiquitous occurrence with injection. The time dependence of T_e, and especially its return after injection to the preinjection level, is characteristic of discharges in which the impurity concentrations are unchanged by injection. In cases with metallic limiters, where impurity radiation in the core commonly rises sharply during injection, T_e returns, after injection is stopped, to a lower value than before. Figure 8 shows the ω_{ce} measurement of the highest T_e achieved; with 2.4 MW of D^0 injected into an H^+ plasma with $\bar{n}_e = 1.9 \times 10^{13}$ cm^{-3}, the central T_e reaches a value greater than 4.0 keV. Significantly, all our measurements indicate that even though the amplitude of the $T_e(r)$ profiles increases during injection, their shape changes fairly little. Despite considerable scatter in the electron heating efficiency, it appears that under optimum conditions with titanium gettering and carbon limiters, T_e increases by about 0.6 eV per kilowatt of injected power.

Ion and Electron Power Balance

To better understand the significance of these results, we performed time-independent numerical calculations of the ion and electron radial power flows with and without injection. Based on the measured radial profiles of electron density and electron temperature, a Monte Carlo beam orbit calculation (*14*) follows the orbits and slowing down of many beam ions and gives the power transferred to the bulk plasma ions, P_{bi}, and to the electrons, P_{be}. It also gives the power lost through beam ions that exchange charge with background neutrals before thermalization and accounts for escaping beam neutrals that are reionized before they leave the plasma. This calculation also gives the power loss associated with beam ions which are scattered into orbits that take them out of the plasma. Using $P_{bi}(r)$ from this calculation, we then determine the radial dependence of the ion temperature, $T_i(r)$, on the basis of neoclassical thermal conduction, ion-electron coupling, and empirical thermal convection and charge exchange loss, as in (*15*). Uncertainties in the radial profiles of impurities, neutrals, and plasma current result in a rather large range of predictions based on these calculations. Varying the unknown parameters over reasonable ranges, we find the corresponding range of the prediction of $T_i(r)$.

The $T_i(r)$ profile predicted in this way is shown in Fig. 9 for a case of 2.1-MW D^0 injection into a low-density $[n_e(0) = 4.5 \times 10^{13}$ $cm^{-3}]H^+$ plasma [$n_e(0)$ is the electron density at the center of the plasma]; experimentally measured points are shown for comparison. The range of prediction indicated by the error bar is 4.0 to 7.5 keV, where the profile shown has been fit to the central temperature measured by charge exchange. The difference between the iron and hydrogen temperatures, estimated to be 800 eV near the center in this case, has been subtracted from the Fe Doppler broad-

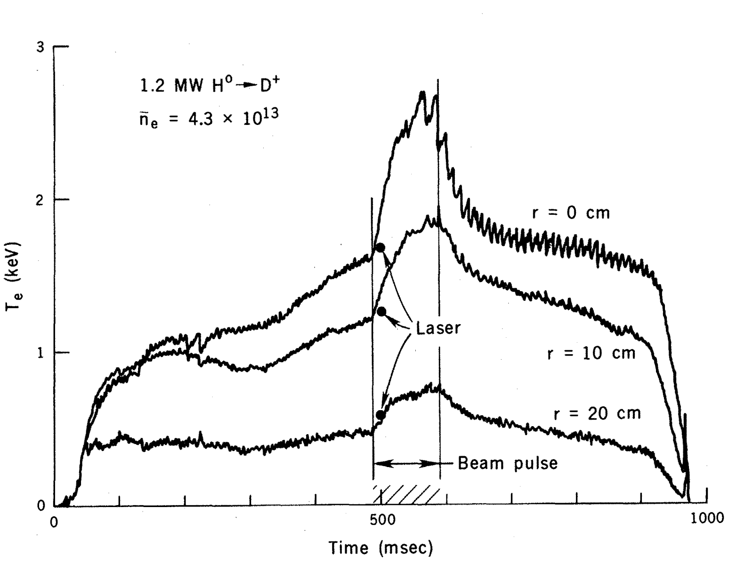

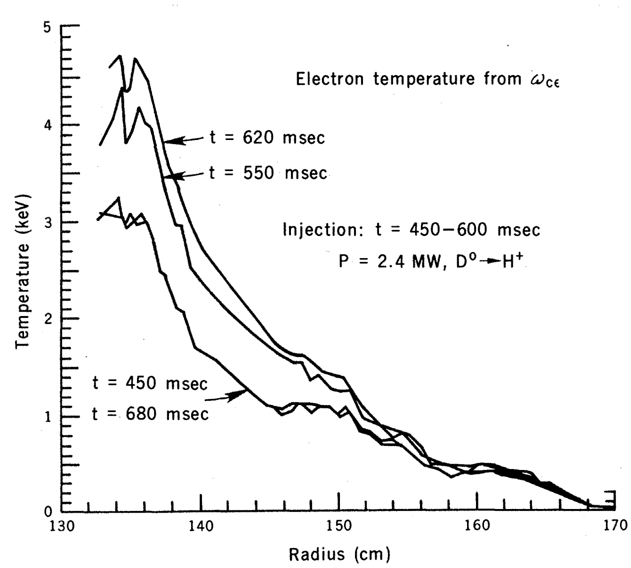

Fig. 7 (left). Electron temperature from $2\omega_{ce}$ at three radial positions during D^+ discharges ($\bar{n}_e = 4.3 \times 10^{13}$ cm^{-3} at the end of the beam pulse) with injection of a 100-msec, 1.2-MW H^0 pulse starting at 490 msec. Also shown are the corresponding values of T_e at a particular time as obtained with the laser Thompson scattering. Fig. 8 (right). Central electron temperature from ω_{ce} measurement with injection of ≈ 2.4 MW of D^0 into an H^+ plasma with $\bar{n}_e = 2 \times 10^{13}$ cm^{-3}. The plasma center is at 134 cm.

ening measurements. The volume-integrated net ion energy confinement time, τ_{Ei}, defined as the thermal energy content of the plasma divided by $P_{bi} - P_{ie}$, where P_{ie} is the power flow between the bulk ions and electrons, is 25 msec for the best fit to the data during injection and about 50 msec during the ohmically heated phase well after the end of injection. In the calculation, this difference arises primarily from the enhanced particle convection and charge exchange loss at high ion temperatures and steep temperature gradients. The reduction in π_{Ei} during injection is thus consistent with our neoclassical model, which includes empirical convective and charge exchange losses. However, because transport due to neoclassical diffusion is only a small fraction of the total energy flow in this case, we cannot rule out an enhancement of the ion thermal conduction by as much as a factor of 5 over the neoclassical value, which is itself uncertain by nearly as large a factor due to uncertainties in the radial distribution of impurities and current. In cases of injection into higher-density plasmas [2.0 MW of D^0 into an H^+ plasma with $n_e(0) = 7.5 \times 10^{13}$ cm^{-3}], the charge exchange and convective losses are greatly reduced, and ion-electron coupling (which we can accurately calculate) dominates the ion energy flow. The maximum credible enhancement of the ion thermal conduction over the neoclassical value in these cases is no greater than a factor of 3 to 4.

Using parameters that predict $T_i(r)$ profiles in good agreement with the measured points, we calculate the power flow between ions and electrons. The beam orbit calculation gives $P_{be}(r)$, the power flowing from the beam ions to the electrons, and $P_{\dot{n}e}(r)$, the power required to thermalize the cold electrons that accompany the beam ions into the plasma. We calculate the ohmic heating profile, $P_{OH}(r)$, from the measured $T_e(r)$ profile, assuming that the radial distribution of impurities is uniform and constant in time and that the plasma conductivity varies as $T_e^{3/2}$. The radiated power, P_{rad}, is scaled from the bolometer measurements.

We define the net electron energy confinement time, $\tau_{Ee}(r)$, as the electron thermal energy inside a radius r divided by $(P_{OH} + P_{be} + P_{ie} - P_{\dot{n}e} - P_{rad})$. During the ohmically heated phase, $P_{be} = 0$ and the sign of P_{ie} reverses. Figure 10 shows $\tau_{Ee}(r)$ for the same case as Fig. 9 (2.1 MW of D^0 injected into a low-density H^+ plasma) both during and well after injection. After injection, $n_e(0)$ drops by 40 percent under these conditions,

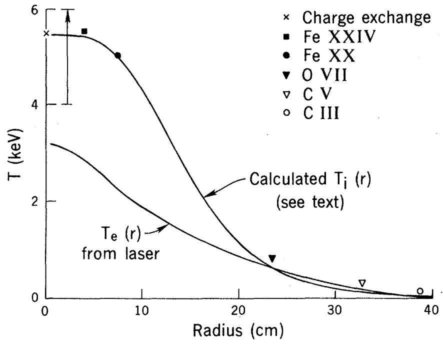

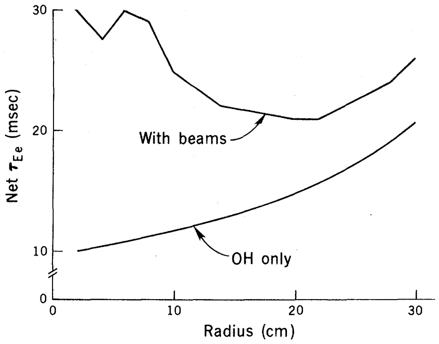

Fig. 9 (left). Calculated ion temperature profile with central value calibrated to experimental data for injection of 2.1 MW of D^0 into a low-density ($\bar{n}_e = 2 \times 10^{13}$ cm^{-3}) H^+ plasma. Fig. 10 (right). Radially integrated net electron energy confinement time for the same case as Fig. 9; *OH* refers to ohmic heating.

but $\bar{n}_e$ is approximately constant. It is noteworthy that, although the net τ_{Ee} for the total plasma is unchanged (within the 30 to 40 percent accuracy of these calculations) during injection, the energy confinement in the central plasma appears substantially enhanced. The direct heating of electrons by the beam and the indirect heating by ion-electron collisions are both relatively weak in the central plasma because of the high electron temperature there, and yet the central temperature rises in proportion to the temperature halfway out, where far more power is transferred to the electrons by beam and plasma ions. If χ_e, the electron thermal conduction coefficient, were unchanged during injection, then since the beam plus ohmic heating is much broader than the initial ohmic heating alone, we would have expected the T_e profile also to broaden and the net τ_{Ee} to decrease. Instead, from the experimental results, we infer a substantial reduction in χ_e in the hot central plasma, as shown in Fig. 11, where

$$\chi_e = \frac{P_{con}}{4\pi^2 R_0 r n_e dT_e/dr}$$

P_{con} being the power carried by electron conduction and convection. Calculating a gross $\tau_{Ee}(a)$ at the limiter for this discharge, where we do not subtract off P_{rad}, yields $\tau_{Ee} = 14$ msec for both the beam-heated and ohmically heated cases—a typical value for low-density gettered PLT discharges. We obtain similar agreement when we perform these calculations for the higher density plasma ($\bar{n}_e = 3.5 \times 10^{13}$ cm^{-3}). The volume-integrated $\tau_{Ee}(a)$ at the limiter is again effectively unchanged, and as before τ_{Ee} in the central plasma is substantially enhanced during injection, implying a decrease in electron thermal transport in the core.

Although the mechanism responsible for the augmented confinement properties of the core electrons during injection remains obscure at this point, the enhancement does appear to be a clear effect. It seems unlikely, however, that the improved confinement represents a simple linear scaling of χ_e with T_e, in light of the fact that χ_e was not reduced in the outer plasma, which was also heated. Moreover, the apparently T_e-dependent decline of χ_e might also be due to some direct effect of injection on electron transport or of the changed ratio of the ion and electron temperatures.

Our electron thermal conductivity data are summarized in Fig. 12, where the product $n_e\chi_e$ is shown as a function of T_e at different minor radii. Not only does the general trend indicate improved confinement at higher T_e, scaling approximately as $1/T_e$, but that is also the case for each radius individually out to $r = 20$ cm. It is apparent that, at higher T_e, the confinement is significantly better than predicted by conventional "INTOR" scaling (*16*), which is insensitive to temperature. However, the radial profile of the thermal conductivity rises to considerably higher values in the outer half of the plasma. It is noteworthy that at the smaller radii in the plasma core and at the higher initial electron temperatures, $n_e\chi_e$ tends to drop during injection. Since n_e generally rises somewhat during injection, the drop in $n_e\chi_e$ implies that the electron energy confinement is improving substantially for these cases.

Plasma Rotation

Since the neutral beam ions carry momentum as well as energy, one would expect unbalanced injection to result in toroidal rotation of the plasma. In previous injection experiments on tokamaks, such rotation has appeared anomalously slow compared to the predictions of neoclassical theory. We studied this problem on

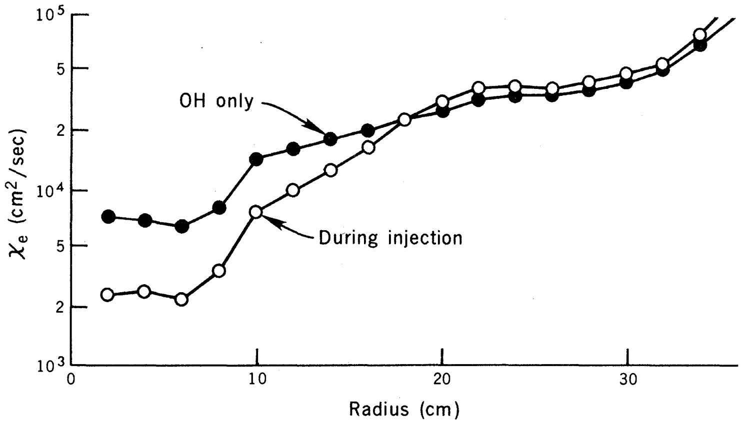

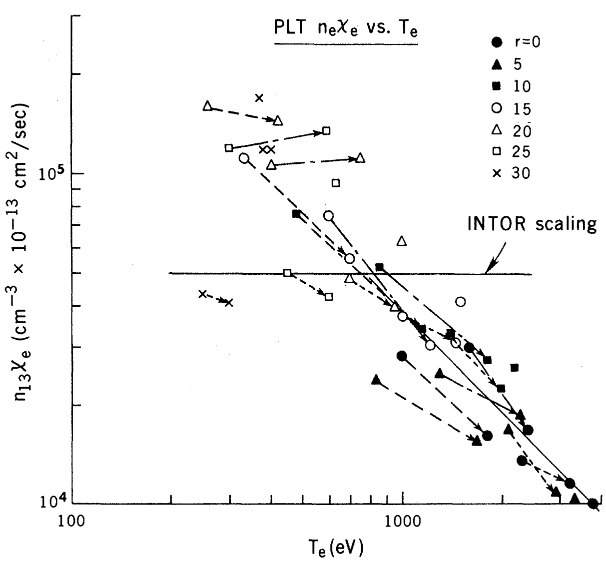

Fig. 11 (left). Electron energy conductivity as a function of radius for the same case as Fig. 9. Fig. 12 (right). Calculations of the product of plasma density and electron thermal transport as a function of electron temperature. Within the central region, both T_e and $n_e\chi_e$ vary by factors of 3 at a given radius. The horizontal line indicates the prediction of the scaling law used in the preliminary studies of the INTOR tokamak. The dashed lines connect points from similar discharges without (left) and with (right) neutral injection.

the PLT by three different methods and found clear evidence of rotation. The methods used were measurement by x-ray wave detector arrays of the phase velocity of the precursor oscillations associated with internal disruptions (sawtooth oscillations), measurement of the tangential charge exchange flux to deduce a shifted Maxwellian ion distribution, and measurement of the Doppler shift of impurity radiation.

All three techniques indicate that with unidirectional injection (either co- or counterinjection) the central plasma rotates at velocities up to 1×10^7 to 1.3×10^7 cm/sec. In the center, the momentum containment time appears to be comparable to the ion energy confinement time. A radial profile of the rotation velocity, obtained from the Doppler shift of radiation from various impurity species (the only technique of the three with spatial resolution), indicates that it drops to the detection limit ($\sim 1 \times 10^6$ cm/sec) near the plasma edge. This rotational profile still corresponds to strongly anomalous viscosity considerably greater than expected from neoclassical theory, but for the first time this tokamak transport coefficient is open to detailed investigation.

Energetics

During high-power injection the average ion energy in the central plasma is high because of the considerable density of slowing-down beam ions there—a consequence of the fact that a beam ion executes many transits of the torus before thermalizing. For instance, in the case of 2.1-MW D^0 injection into an H^+ plasma with $\bar{n}_e = 2.3 \times 10^{13}$ cm^{-3}, our Monte Carlo calculation indicates that the density of slowing-down beam ions on axis is 1.2×10^{13} cm^{-3}, with an average energy of 19 keV, while the corresponding bulk plasma ion density is 2.5×10^{13} cm^{-3}, with an average energy of 8.25 keV on axis. The calculated average ion energy on axis is thus about 12 keV, and Γ, the ratio of energy in the slowing-down beam ions to that in the thermal plasma, is 0.7. It is reassuring that the presence of so much energy, both thermal and nonthermal, does not appear to provoke any instabilities serious enough to significantly enhance energy loss from the plasma.

Operating with 2.2-MW D^0 injected into a D^+ plasma, we achieved 2×10^{13} neutrons per pulse and a maximum neutron yield of $\approx 1.6 \times 10^{14}$ per second, corresponding to a fusion output power of about 170 W. Allowing for the much larger deuterium-tritium fusion cross sections and the greater energy release per reaction, the same set of conditions with D^0 injection into a T^+ plasma would be expected to yield 50 kW of fusion power.

Although the PLT was not designed to produce power efficiently, it is nonetheless of interest to compare the input and output powers. If one defines a parameter Q_p as the ratio of equivalent fusion power in deuterium-tritium plasma operation to the plasma heating power, then Q_p in the case above is 2 percent, since the total heating power was about 2.5 MW (2.2 MW of beam power and about 0.3 MW of ohmic power during injection)—much the highest Q_p ever achieved in a fusion experiment. While this is encouraging, some qualifications should be kept in mind. Most of the neutrons (> 90 percent) result not from reactions of the thermal ions with each other, but from reactions of the beam ions with each other and with thermal ions. This is very similar to the situation that would obtain in a driven subignition fusion reactor, but not in an ignited thermonuclear reactor (where after ignition all the neutrons would result from reactions among thermal ions).

Further, while the plasma received only 2.5 MW of heating power, the total raw power drawn off the line was much greater: the neutral injectors, only about one-third efficient, consumed more than 6 MW, the ohmic heating transformer used about 20 to 30 MW inducing the plasma current, and the toroidal field coils used 150 to 200 MW. Extrapolating to a fusion reactor, we note that since the beams would operate only transiently during the ignition phase in a self-sustaining thermonuclear reactor, the inefficiency of the injectors would not present a serious problem. This inefficiency could hamper a beam-driven subignition reactor, but only if the technology to improve beam efficiency at high energies by direct recovery of unneutralized ions or use of negative ions fails to mature. The poor efficiency of the ohmic transformer is due to the extremely reactive design chosen for the PLT; the power drawn by this transformer is nearly independent of the plasma current loading it, and such inefficiency would not be mandatory in a fusion reactor. The use of superconducting ohmic transformer coils would eliminate their resistive loss, while the excess reactive energy could be minimized and largely recovered. The third factor, the enormous power consumption of the toroidal field coils, is not really relevant, since a practical fusion reactor would almost certainly use superconducting coils. Thus, when viewed in context, our definition of Q_p appears reasonable for judging the proximity to reactor conditions, taking into account the fact that an economical pure fusion reactor would need to operate at $Q_p \gtrsim 10$, to compensate for the ~ 30 percent efficiency in converting neutron energy to electricity.

Conclusion

Using neutral beam injectors developing a total power of as much as 2.4 MW, we reached central ion temperatures as high as 6.5 keV and central electron temperatures $\gtrsim 4.0$ keV, both the highest yet achieved in a tokamak device. During D^0 injection into a D^+ plasma, the equivalent D-T energy gain factor Q_p reached 0.02, the maximum reached in a controlled fusion experiment. At the highest temperatures and lowest densities, the ion collisionality parameter, ν_i^*, reached a minimum of ~ 0.02 and was below 0.1 over much of the plasma, for the first time well into the collisionless regime relevant to reactors, yet the ion thermal conductivity appeared consistent with neoclassical theory within our uncertainties of a factor of 3 to 5. Indeed, the temperatures reached would not have been possible with the available injection power had the direst predictions of anomalous transport theories obtained. Agreeably, and somewhat surprisingly, the electron thermal conductivity appeared to be suppressed in the central plasma during high-power injection. Under some conditions, impurity radiation seriously degraded the electron energy confinement, but the severity of the impurity problem was substantially reduced by the use of graphite limiters. Unbalanced injection engendered rotation of the plasma core, and new density fluctuations were observed at the lower collisionalities (corresponding to higher values of $P_b/\bar{n}_e$), but neither phenomenon appeared to deleteriously affect stability or energy containment. Without exception, these findings are encouraging regarding the practicality of fusion as a power source.

References and Notes

1. H. P. Furth, *Nucl. Fusion* **15**, 487 (1975).
2. D. L. Dimock, D. Eckhartt, H. P. Eubank, E. Hinnov, L. C. Johnson, E. B. Meservey, E. L. Tolnas, D. J. Grove, *Proc. 4th Int. Conf. Plasma Phys. Controlled Nucl. Fusion Res.* **1**, 451 (1971).
3. J. G. Cordey, J. Hugill, J. W. M. Paul, J. Sheffield, E. Speth, P. E. Stott, V. I. Tereshin, *Nucl. Fusion* **14**, 441 (1973).
4. K. Bol *et al.*, *Proc. 5th Int. Conf. Plasma Phys. Controlled Nucl. Fusion Res.* **1**, 77 (1975).
5. L. A. Berry *et al.*, *Proc. 6th Int. Conf. Plasma Phys. Controlled Nucl. Fusion Res.* **1**, 49 (1977).
6. Equipe TFR, *ibid.*, p. 69.
7. J. W. M. Paul *et al.*, *Proc. 8th Eur. Conf. Controlled Fusion Plasma Phys.* **2**, 49 (1977).
8. V. S. Vlasenkov *et al.*, *Proc. 6th Int. Conf. Plasma Phys. Controlled Nucl. Fusion Res.* **1**, 85 (1977).
9. J. G. Cordey, *Proc. 5th Int. Conf. Plasma Phys. Controlled Nucl. Fusion Res.* **1**, 623 (1975).
10. J. Killeen and K. D. Marx, in *Methods of Computational Physics*, B. Alder, Ed. (Academic Press, New York, 1970), vol. 9, p. 422.
11. B. Rose, A. E. Taylor, E. Wild, *Nature (London)* **181**, 1630 (1958).
12. J. D. Strachan *et al.*, *ibid.* **279**, 626 (1979).
13. F. L. Hinton and M. N. Rosenbluth, *Phys. Fluids* **16**, 836 (1973).
14. D. L. Jassby and R. J. Goldston, *Nucl. Fusion* **16**, 613 (1976).
15. P. E. Stott, *Plasma Phys.* **18**, 251 (1976).
16. W. M. Stacey, Jr., *et al.*, U.S. INTOR—The U.S. Contribution to the International Tokamak Reactor Workshop, Vienna, 1979.
17. H. P. Eubank *et al.*, *Phys. Rev. Lett.* **43**, 240 (1979).

18. I especially thank R. J. Goldston and H. P. Eubank for many suggestions during the writing of this article and M. B. Gottlieb, E. A. Frieman, and H. P. Furth for their continuous support. This work was supported by U.S. Department of Energy contract EY-76-C-02-3073.

Yakataga Gap, Alaska: Seismic History and Earthquake Potential

William R. McCann, Omar J. Pérez, Lynn R. Sykes

One of the world's major earthquake belts (Fig. 1) follows the boundary between the Pacific and North American plates from offshore British Columbia to southern Alaska and thence to the Aleutian island arc. Most of the movement between the two plates occurs during great earthquakes—events of surface wave magnitude, M_s, greater than 7.8. The repeat time of great shocks along some of the major plate boundaries of the world varies from about 40 to 500 years. Since much of the plate boundary in Fig. 1 ruptured in large shocks during the last 40 years, most of it appears to have a low potential for large shocks during the next few decades.

Nevertheless, Tobin and Sykes (*1*), Kelleher (*2*), and Sykes (*3*) identified four segments of this plate boundary that had not been the locations of large earthquakes for many decades. They concluded that these segments, which they called seismic gaps, were some of the most likely sites of future large shocks. One of the gaps they delimited ruptured in 1972 during the large southeast Alaska earthquake of magnitude 7.6 (Fig. 1).

The locations and magnitudes of at least 12 large earthquakes along some of the simple plate boundaries of the world have been successfully forecast (*4–6*) since Fedotov (*7*) introduced the concept of the seismic gap in 1965. The gap concept by itself, however, does not permit an estimate of the time of occurrence of a future large shock that is precise enough to be called a prediction, which we take to involve precise estimation of time of occurrence, place, and size. Only a small part of the gap in southern Alaska, shown in Fig. 1 near 60°N, 143°W, ruptured during the recent Saint Elias earthquake of M_s 7.7 on 28 February 1979 (*8*). The remaining area, here called the Yakataga seismic gap, its seismic history, and its potential for a future shock are the main focus of this article.

The authors are at Lamont-Doherty Geological Observatory of Columbia University, Palisades, New York 10964. William McCann and Omar Pérez are research assistants at Lamont-Doherty and graduate students at Columbia University. Lynn Sykes is a professor of geology at Columbia University.

Repeat Times of Large Earthquakes

In southeast Alaska and along offshore British Columbia, motion between the Pacific and North American plates is accommodated by right-lateral strike-slip motion (*1*) such that the Pacific plate moves in a N15°W direction (heavy arrows in Fig. 1) with respect to North America (*1*, *9*, *10*). Farther west, the Pacific plate is thrust (subducted) beneath the North American plate along the Aleutian trench. The Yakataga gap is located in a transition zone between these two regimes of plate interaction.

In southern Alaska the computed rate of plate movement is about 6 centimeters per year (*9*, *10*). Thus, about 5 meters of

0036-8075/80/0321-1309$01.25/0